Wideband MIMO Antenna for 5G Base Station

Hien Doan Thi Ngoc*

Abstract—In this paper, we present a configuration of a wideband MIMO antenna array for 5G terminals. The single-element antenna has compact size, dual polarization, wide operating bandwidth covering the 5G N78 frequency band, and high isolation between the two input ports (>40 dB). The 4×1 radiation sub-array has dual polarization, low mutuality and high spatial diversity characteristics over the entire operating frequency range. The large-scale MIMO antenna array with a single 4×8 configuration can provide 8 independent beams azimuth sweep and 8 independent beams sweep azimuth. When exciting all ports in either horizontal or vertical bias, a large-scale MIMO antenna array can produce a main beam with a maximum realized gain of about 22 dBi. With many advantages of low profile, wideband, low mutuality, this large-scale MIMO antenna array can be applied to the current generation of 5G mobile base stations.

Index Terms—MIMO antenna, wideband, array antenna.

1. Introduction

The next generation mobile network 5G has been tested and commercialized around the world. The number of terminals supporting 5G is increasingly popular around the world, leading to extremely large requirements for data speed, latency, and bandwidth. For the equipment system of the 5G generation mobile communication network, the antenna for the base station is a very important component to help the system meet the requirements of bandwidth, speed, anti-interference ability, etc. As a result, 5G technology satisfies the demand for high-speed mobile broadband services, capable of supporting HD, 4K UHD video and other rich content services. In general, the optimal design of large-scale MIMO antennas is both capable of performing well in the 5G frequency band, has a gain suitable for the application, and ensures MIMO characteristics such as isolation, radiation correlation,... will be great challenges for researchers today. Currently, as 5G networks have been tested and commercialized globally, large-scale MIMO antenna studies are still of considerable interest. With more than 100 antennas deployed at the mobile base station, large-scale MIMO antennas present significant challenges. An active multi-beam antenna system for large-scale 5G MIMO networks is designed and implemented in [1], which consists of 64 RF channels and a 64-element antenna array evenly distributed on eight printed PCB boards. The size of each individual printed circuit board (PCB) is 320 mm × 215 mm ($6\lambda \times 4\lambda$), where λ is the wavelength in free space). The antenna array resonates at 5.8 GHz and has an impedance bandwidth of 200 MHz. The results of simulation and measurement of the gain of the antenna array are 13 and 11 dBi, respectively.

In [1], a system integrating EM lens with large array is capable of focusing the energy of any incident plane wave passing through the EM lens to a small focal area of the antenna array, depending on the angle of incidence of the wave. In [2], [3], a practical 2-D printed circuit antenna array configuration for MIMO systems has been proposed. The 1×4 sub-antenna array has a gain of 11.7 dBi. The MIMO antenna array consists of 8 × 4 subarrays of size $4\lambda \times 8\lambda$, with a gain simulation of 15 dBi. The stacked printed circuit antennas shown in [4]–[7] are low profile. The radiation plate is powered through an orthogonal slot [4]–[6] double polarized radiation with high isolation. In [7], the capacitive coupling technique was proposed for the design of 1800 MHz GSM network antennas with dual polarization and high isolation. However, in these studies each radiation plate needed a separate galvanic structure to achieve double-polarized radiation.

This paper introduces a wideband MIMO antenna array structure for a 5G base station consisting of a single element antenna, a 4 × 1 sub-antenna array, and a large-scale MIMO antenna. The single element antenna structure has a compact size, bandwidth covering the 5G N78 band, and a high isolation between the two input ports (>40 dB). The 4 × 1 radiation sub-array has dual polarization, low mutuality over the entire operating frequency range. The large-scale MIMO antenna array with a single 4×8 configuration can provide 8 independent beams azimuth sweep and 8 independent beams sweep azimuth. When exciting all ports in either horizontal or vertical polarization, the large-scale

Hien Doan Thi Ngoc is with Faculty of Communication Engineering, School of Electrical and Electronic Engineering, Hanoi University of Science and Technology.

**Corresponding author: Hien Doan Thi Ngoc (e-mail: hien.doanthingoc@hust.edu.vn)*

Manuscript received March 28, 2023; revised April 11, 2023; accepted June 02, 2023.
Digital Object Identifier 10.31130/jst-ud.2023.105

MIMO antenna array can produce a main beam with a maximum realized gain of about 22 dBi.

2. Antenna Design

2.1. Single element antenna design

The configuration of the single element antenna is shown in Fig. 1. The single element antenna is designed on PCB printed circuit technology including 7 layers: 3 dielectric layers FR4 (ϵ_r = 4.4; tanδ = 0.02) and four layers of metal. The feeding network consists of two Wilkinson dividers printed on the top side of dielectric layer 1 (Sub#1, $h_1 = 1mm$) and apeture coupled through 4 narrow slots on the ground plane printed on the bottom side of dielectric layer 1 by using open-circuit stubs have length $L_s = 8.5mm$, width $W_s = 1.9mm$ (Fig. 1b). Four microstrip lines with dimensions $a_2 = 15.7mm$ and $b_2 = 1.6mm$ are printed on the top side of dielectric layer 2 (Sub#2; $h_2 = 1.6mm$). A square array of 2×2 radiation plates with dimensions $a_1 = b_1 = 17mm$ is printed on the top face of dielectric layer 3 (Sub#3; $h_3 = 1.6mm$), the center line connecting the radiators has length $D_1 = D_2 = 31.5mm$. The dielectric layers are stacked and fixed together with 4 pairs of plastic screws. Four microstrip lines are placed on the line connecting the centers of adjacent pairs of radiators. The antenna is fed directly via two standard 3.5 mm 50Ohm SMA connectors at the inputs of two Wilkinson dividers. These two SMA connectors are soldered perpendicular to the underside of Sub#1 to facilitate the placement of elements when coupling large-scale MIMO arrays. The overall dimensions of the antenna are 75.0 mm $\times$ 80.0 mm $\times$ 4.2 mm. The antenna was simulated using HFSS software in the ANSYS Electromagnetic Suite. The dimension parameters of single element antenna are listed in Tab. 1. The energy coming from the two input ports is split in half through a Wilkinson divider, routed through two narrow slots in the ground plane, and then coupled to a microstrip line crossed above the slots. Each terminal of the divider, the gap and the coupling microstrip line act as a feeding for the two radiators by capacitive coupling. So, the Port #1 excites a steady and co-phase current along the x-axis on all four radiation plates, and Port #2 excites a steady and co-phase current along the y-axis, as shown in Fig. 2. Horizontal polarization and TM01 mode polarization of the four radiators are generated independently when feeding Port #1 or Port #2. The advantage of the antenna symmetrical arrangement is the ability to increase isolation between the horizontal and vertical polarization.

The feeding network of single element antenna consists of two Wilkinson dividers to provide power through four narrow slots in the ground plane. The design model of the Wilkinson divider circuit is shown in Fig. 3. The input impedance of the feeding circuit is $Z_0 = 50\Omega$, the impedance of the Wilkinson bridge is $Z_1 \sim 70.7\Omega$; Wilkinson bridge is rectangular in shape. The feeding circuit is designed on a 1 mm thick layer of dielectric material FR4 ($\epsilon_r = 4.4$; tanδ = 0.02), operating at a center frequency of 3.6 GHz; microstrip width of 50 Ω and microstrip of 70.7 Ω are $WZ_0 = 1.9mm$, respectively; $WZ_1 = 1.0mm$. The isolation 100 Ω resistor is used in the design.

TABLE 1: Optimized design parameters of the single element antenna (Unit: mm)

Parameter	Value (mm)	Parameter	Value (mm)
a_1	17.0	h_1	1.0
a_2	15.7	h_2	1.6
a_3	1.0	h_3	1.6
b_1	17.0	L	75.0
b_2	1.6	L_s	8.5
b_3	12.2	W	80.0
D_1	31.5	W_s	1.9
D_2	31.5	WZ_0	1.9
t	13.75	WZ_1	1.0

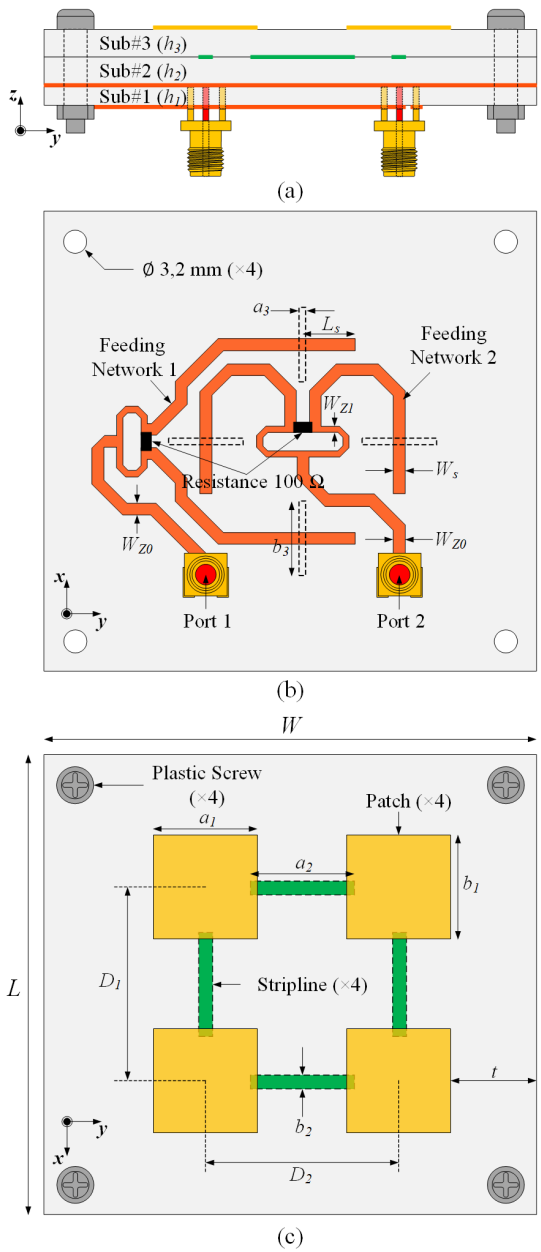

Fig. 1: Single element antenna configuration: (a) Side view, (b) Bottom view of Sub#1 và (c) Top view of Sub#2 và Sub#3

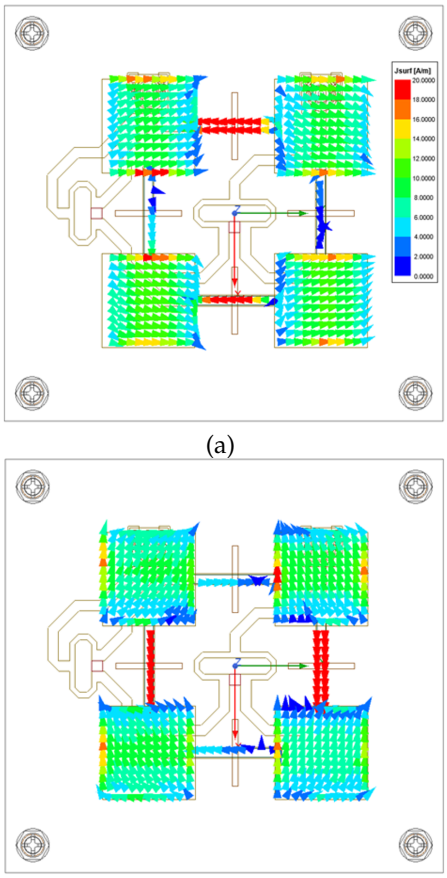

Fig. 2: Surface current distribution on the radiators: (a) Horizontal polarization when the Port #1 excited and (b) Vertical polarization when the Port #2 excited.

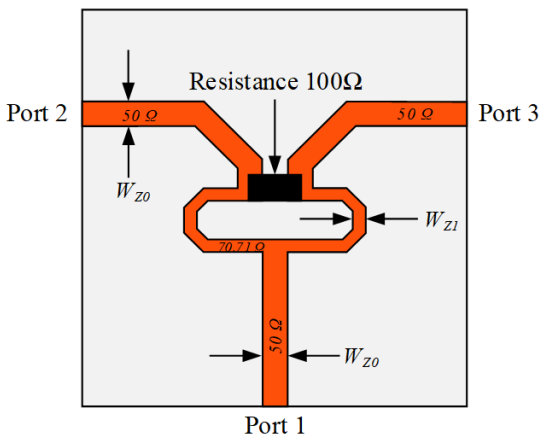

Fig. 3: Wilkinson feeding network model

Input impedance bandwidth |S11| < -20 dB of Wilkinson divider reached 31.84% (3.01 – 4.15 GHz), |S11| is -41.29 dB at the frequency of 3.6 GHz. The power at the two output ports is about 44.7% of the input power (-3.5 dB). The isolation between the two output ports reaches 21.62 dB at the frequency of 3.6 GHz. The simulation results of S parameters of Wilkinson divider are shown in Fig. 4.

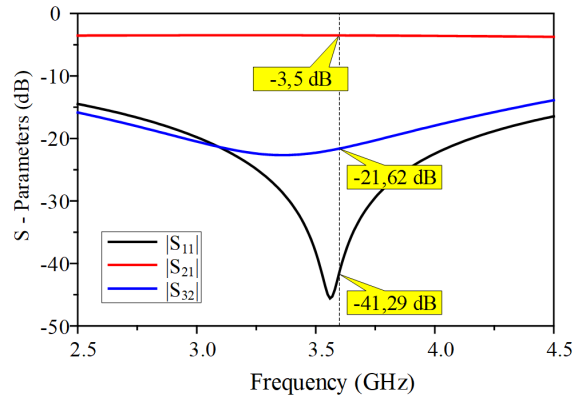

Fig. 4: S-parameters simulation results of Wilkinson divider

Fig. 5 illustrates the simulation results of the S parameter of a single element antenna, the input impedance bandwidths of the two ports (|Sii| < -15 dB) almost coincide. Input impedance bandwidth |S22| < -15 dB at Port #1 reached 11.27% (3.35 – 3.75 GHz), and is -22.40 dB at the frequency of 3.6 GHz. Input impedance bandwidth |S22| < -15 dB at Port #2 reached 10.67% (3.37 – 3.75 GHz) and is -18.37 dB at the frequency of 3.6 GHz. The overlapping bandwidth of the two antenna ports (|Sii| < -10 dB) covers the N78 5G NR band (3.3 – 3.8 GHz). In the overlapping bandwidth |Sii| < -15 dB isolation between two antenna ports > 35 dB; At 3.6 GHz central operating frequency, the two antenna ports have an isolation level of 62.12 dB. This is due to the multilayer symmetric structure of the antenna and the excitation antenna has two orthogonal polarization modes.

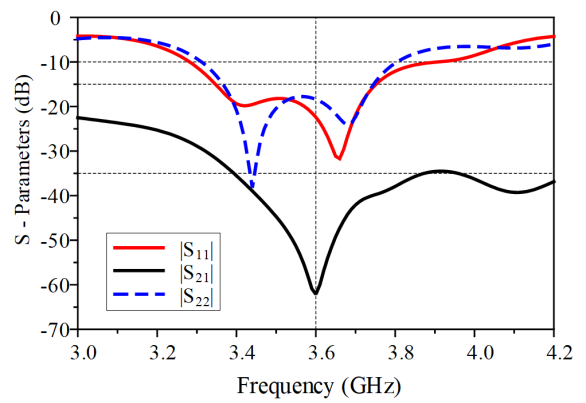

Fig. 5: S-parameter simulation results of single element antenna

The realized gain and radiation efficiency of a single element antenna with respect to frequency are illustrated in Fig. 6. In the operating bandwidth |Sii| < -15 dB, when the Port #1 excited, the antenna's realized gain is from 5.54 to 7.61 dBi, the antenna's radiation efficiency is from 53% to 60%; when the Port #2 excited, the antenna's realized gain is from 5.91 to 6.61 dBi, the antenna's radiation efficiency is from 53% to 62%; when the Port #2 excited. The radiation pattern of a single element antenna at frequencies of 3.5 GHz, 3.6 GHz and

3.7 GHz when the Port #1 and the Port #2 excited respectively is shown in Fig. 7. These results demonstrate that the antenna has a balanced and stable radiation pattern throughout the operating frequency range.

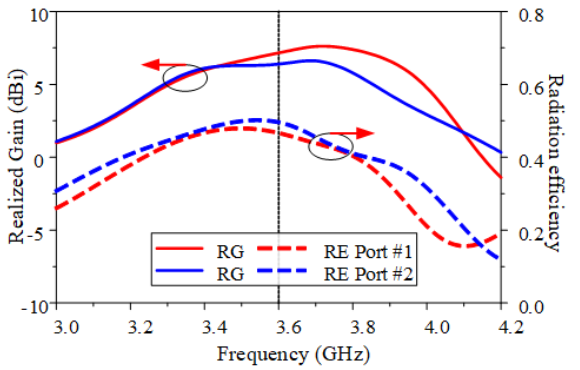

Fig. 6: Realized gain and radiation efficiency of a single element antenna

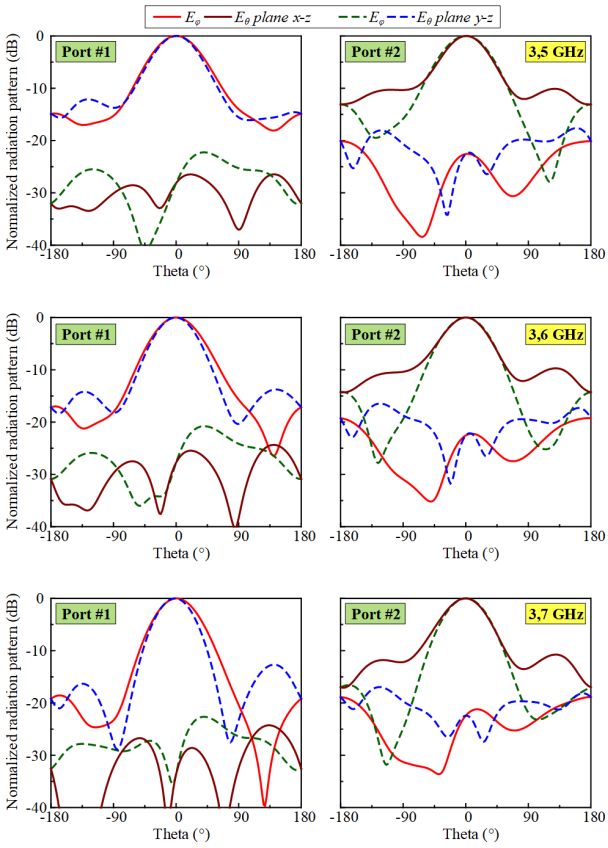

Fig. 7: Radiation pattern of single element antenna at the frequencies of 3.5 GHz; 3.6 GHz and 3.7 GHz

The Altium software is used to design single antenna PCB printed circuit layout. The antenna consists of 3 printed PCBs: A 2-layer PCB for ground and ground planes, a PCB for four microstrip lines and a PCB for 2 × 2 square radiators as shown in Fig. 8a. The PCB circuit after placing the fabrication process on the FR4 material is photographed in Fig. 8b. The PCBs are drilled with 3.0 mm holes at the 4 corners, the hole position is 5.0 mm from the corners. M3 plastic screws are used to fix 3 stacked PCB layers. The overall dimensions of the antenna are 75.0 mm × 80.0 mm × 4.2 mm excluding screws. Two standard 3.5mm SMAs are used to feed the antenna and for convenience during measurement, the SMA is soldered perpendicular to the Sub#1 PCB. A fabricated prototype is shown in Fig. 8b. Fig. 9 shows the measured and simulation results of the proposed antenna. The measured results show that the input impedance bandwidth at Port #1 |S11| < -15 dB reached 11.08% (3.41 – 3.81 GHz), at 3.6 GHz value |S11| determined to be -20.35 dB. Input impedance bandwidth at Port #2 |S22| < -15 dB achieves 12.18% (3.39 – 3.83 GHz), at 3.6 GHz value |S11| determined to be -15.26 dB. In the overlapping bandwidth |Sii| < -15 dB isolation between two antenna ports > 30 dB. At the central operating frequency of 3.6 GHz, the two antenna ports have an isolation level of 42.12 dB.

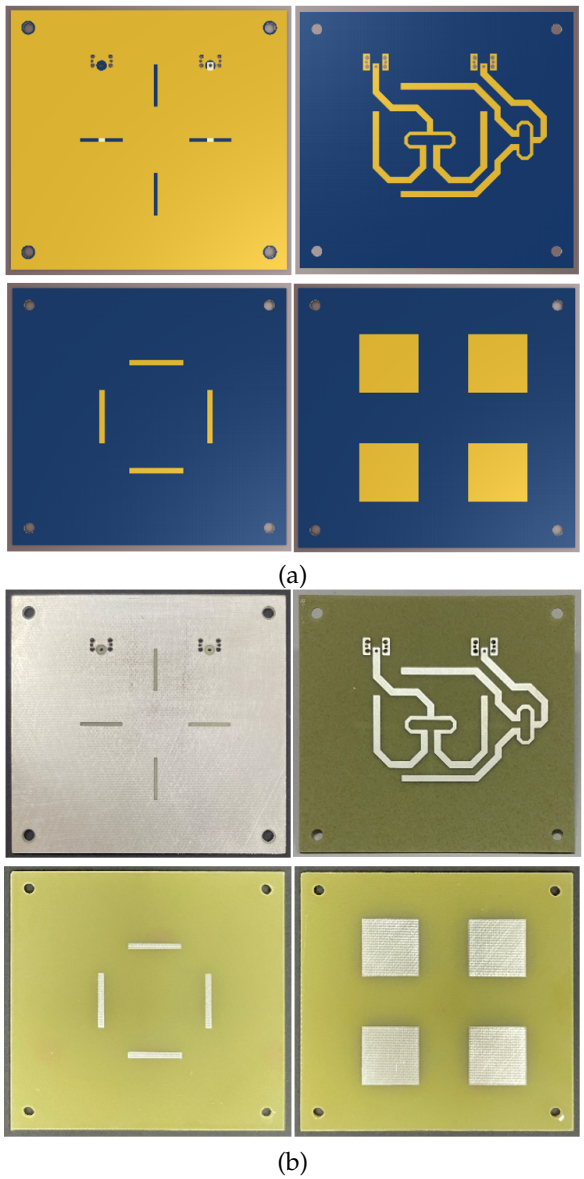

Fig. 8: (a) Printed circuit layout in Altium software and (b) Actual photo of PCB

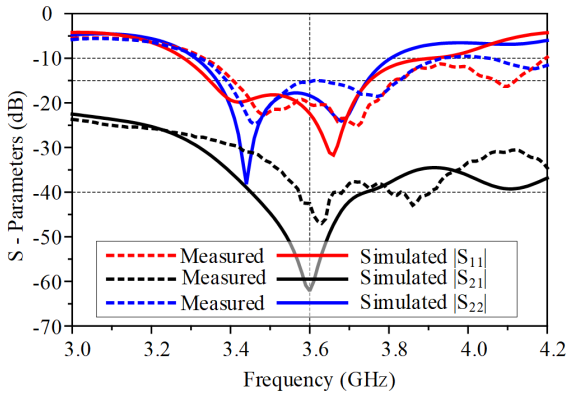

Fig. 9: The results of measurement and simulation of S-parameter of single element antenna

2.2. 4 × 1 sub-array design

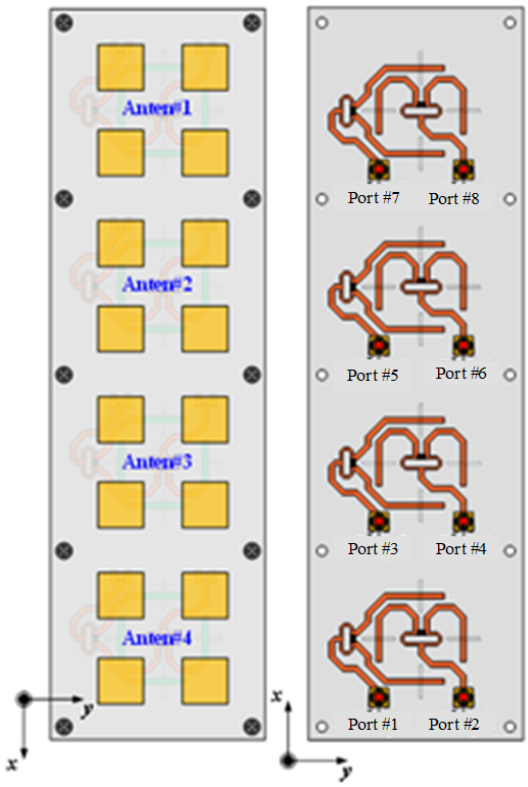

Fig. 10: Design model of 4 × 1 sub-array

A 4 × 1 sub-array was designed by arranging single antennas along the x-axis as shown in Fig. 10, with dimensions of 264.0 mm × 80.0 mm × 4.2 mm. There are eight ports in the subarray, four for horizontal mode (Port #1, #3, #5, #7) and four for vertical mode (Port #2, #4, #6, #8). The sub-array is designed on FR4 dielectric (ϵ_r = 4.4; tanδ = 0.02) exactly as a single antenna element. The distance between the antennas is D = 63 mm. Fig. 11 illustrates the simulation results of the S-parameter of the 8 input ports of the subarray. The input impedance bandwidth of the ports (|Sii| < -15 dB) almost coincides with the simulationed results of the single element antenna. Fig.12a shows the isolation between single antenna ports (Ant#1, Ant#2, Ant#3, Ant#4), in overlapping bandwidth |Sii| < -15 dB isolation between two ports belonging to a single antenna > 35 dB. Mutuality between adjacent antenna ports of the same excitation mode < -25 dB in overlapping bandwidth |Sii| < -15 dB; at 3.6 GHz the port-to-port mutuality < - 28 dB as shown in Fig.12b.

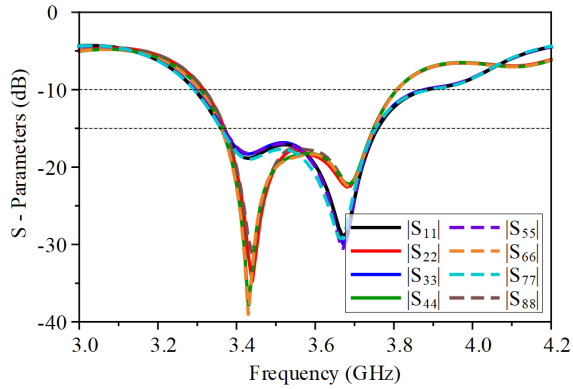

Fig. 11: Input impedance bandwidth of 8 sub-array ports

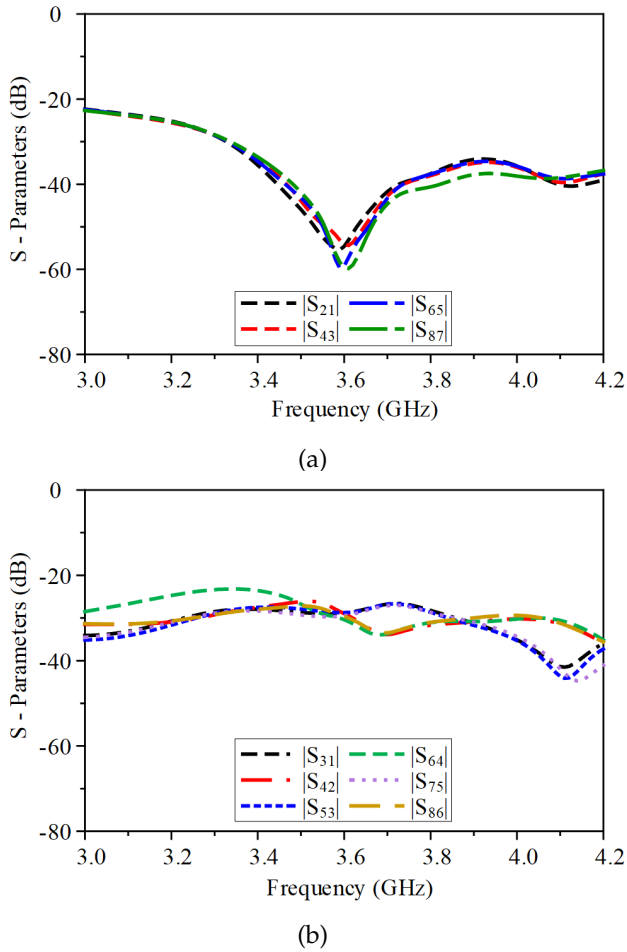

Fig. 12: (a) Simulation results of isolation between single antenna ports and (b) Mutality between adjacent antenna ports of the same excitation mode

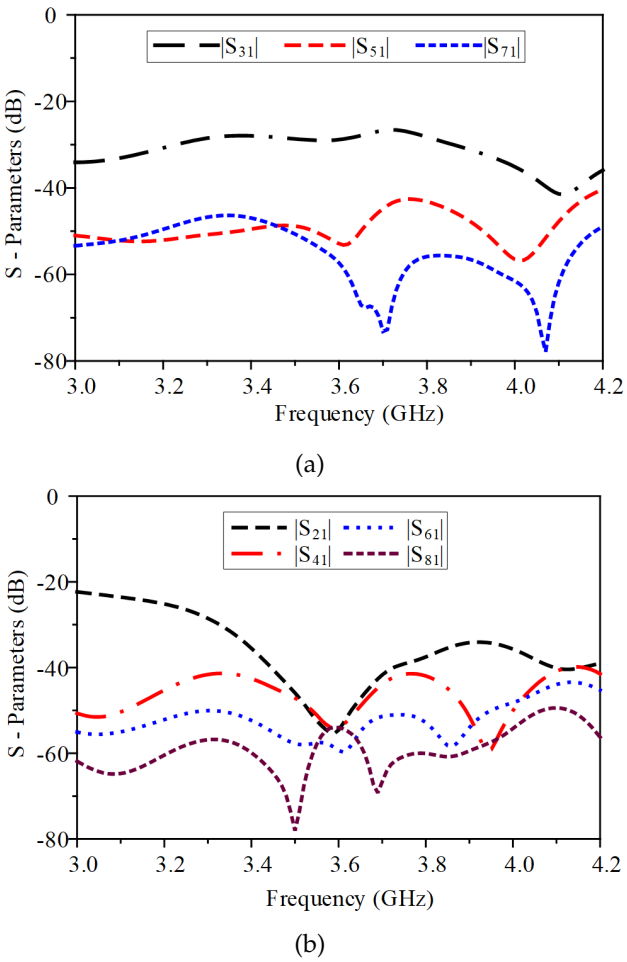

Fig. 13: Mutality between antenna ports in the array is 4 × 1 compared to port 1: (a) Co-polarization and (b) Cross-polarization

Fig. 13 illustrates the simulation results of the mutuality between other ports in the 4×1 subarray with Port #1 belonging to Ant#1. In the operating bandwidth, the co-polarization port mutuality (Port #3, Port #5, Port #7) < -25 dB; At the frequency of 3.6 GHz, this mutuality is determined to be -28.84 dB, -52.90 dB and -57.31 dB, respectively. Cross-polarity port mutuality (Port #2, Port #4, Port #6, Port #8) < - 35 dB in operating bandwidth; at the frequency of 3.6 GHz these mutualities are determined to be -54.60 dB, respectively; -53.98 dB, -59.36 dB, -54.01 dB. As the distance increases, the mutuality between the antenna ports decreases.

The simulation results of the co-polarization and cross-polarization realized gain when feeding each single antenna in the array are illustrated in Fig. 14. When excitation is horizontally polarized, the realized co-polarization gain is determined in the range 5.39 - 7.49 dBi and is 28 dB higher than the cross -polarization as Fig. 14a. When excitation is vertically polarized, the realized co-polarization gain is determined in the range 4.56 –6.57 dBi and 22 dB higher than the cross -polarization as shown in Fig. 14b.

When excitation of the horizontal and vertical polarization of all four single antennas simultaneously, the measured co-polarization gain is 11.41 – 13.39 dBi and 11.06 – 12.59 dBi. The realized co-polarization gain when excitation of the horizontal polarization mode determined at 3.6 GHz is 13.02 dBi, which is similar to that of the vertical polarization mode of 12.47 dBi. Cross-polarization level for horizontal mode excitation is greater than 31 dB and 23 dB for vertical mode excitation.

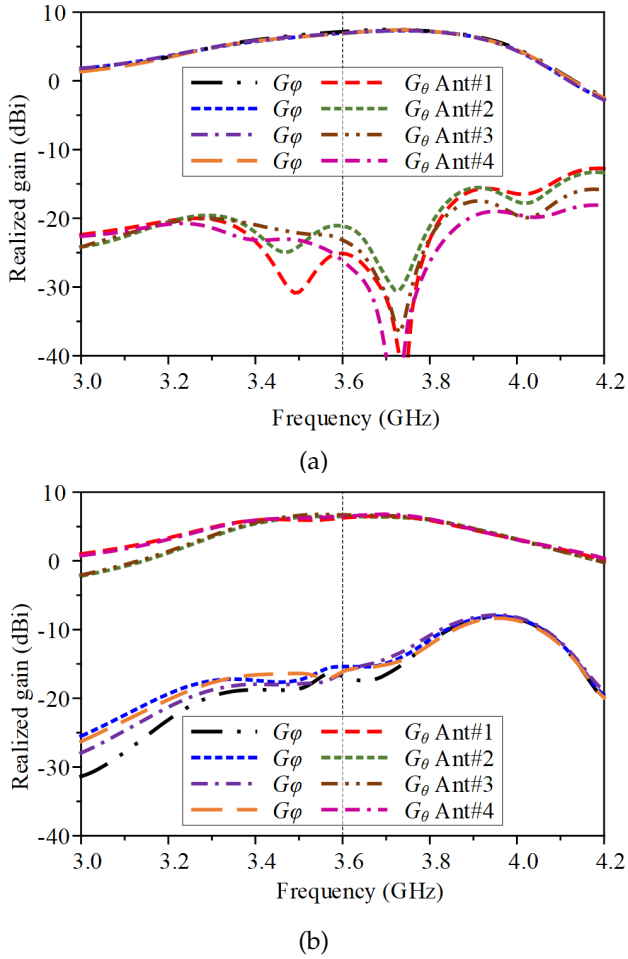

Fig. 14: Simulation results of the realized gain of co-polarization and cross polarization when excitation of single antennas: (a) Horizontal polarized excitation, (b) Vertically polarized excitation

Fig. 16 illustrates the radiation of the subarray excitation in horizontal and vertical polarization modes. When excitation of the horizontal polarized mode, the half-power beam width (HPBW) at the frequencies of 3.5 GHz, 3.6 GHz and 3.7 GHz in the x-z plane was determined to be 16.98°, respectively; 16.53° and 16.00° and in the y-z plane 59.51°; 54.54° and 50.42°; F-B ratio > 15 dB and cross polarization level is greater 31.52 dB. When exciting Port #2, the antenna radiates vertically polarized, half-power beam widths (HPBW) at the frequencies of 3.5 GHz, 3.6 GHz and 3.7 GHz in the determined x-z plane, respectively, is 16.15°; 16.10° and 16.04° and in the y-z plane are 61.25°, respectively; 59.87° and 58.77°; F-B ratio > 13 dB and cross polarization level is greater 22.65 dB.

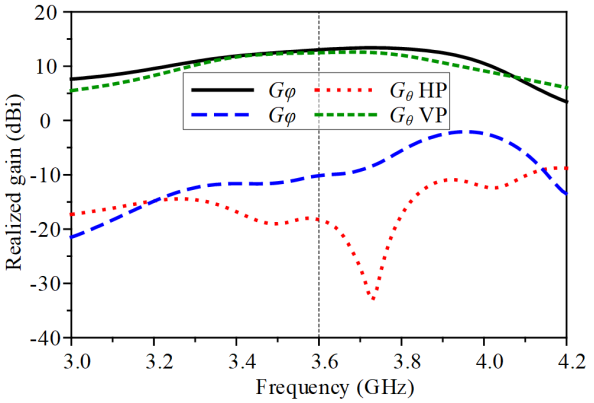

Fig. 15: Co- polarization and cross-polarization realized gain of subarray when excitation of horizontal and vertical polarization all 4 single antennas simultaneously

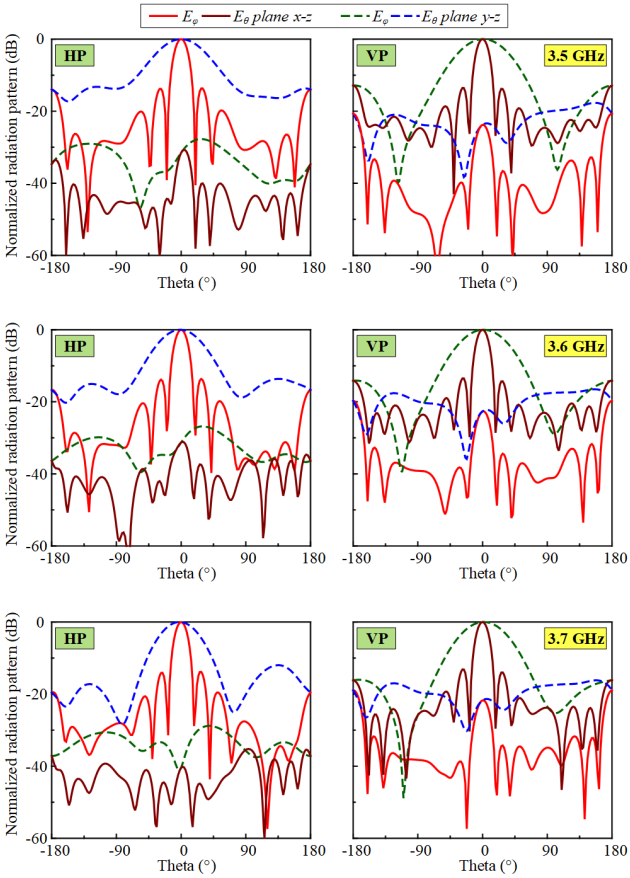

Fig. 16: Radiation pattern of the subarray when excitation in horizontal and vertical polarization modes

2.3. Large-scale MIMO array antenna

The large-scale MIMO array antenna configuration for the base station is shown in Fig. 17. The structure of the array consists of 4×8 single antenna elements and is assembled from 8 4×1 sub-arrays. The distance between single elements in the x-axis is 63 mm, the distance in the y-axis is 80 mm. The array consists of 32 single antennas, 64 feeding ports (32 horizontal-mode excitation ports and 32 vertical-mode excitation ports), 64 Wilkinson relay networks, and 256 printed radiators.

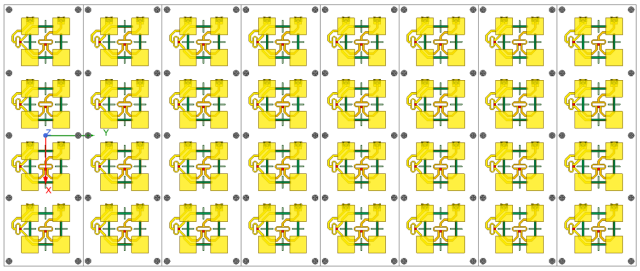

Fig. 17: Design model of large-scale MIMO antenna array 4×8

The simulation results show that the antennas in the large-scale MIMO array have the same performance as the single antenna element and the 4 × 1 sub-array with wide operating bandwidth characteristics |Sii| < - 15 dB approximately 10%, bandwidth overlap |Sii| < -10 dB covers the 5G NR N78 frequency band.

The mutuality between the antenna ports in the array is very low due to the almost perfect symmetry of the radiated elements, the microstrip lines of the single antenna element. Configuration of 4×8 single antennas, 264 mm×640 mm×4.2 mm overall size, large-scale MIMO array can provide 8 azimuth sweep independent beams and 8 azimuth sweep independent beams elevation angle.

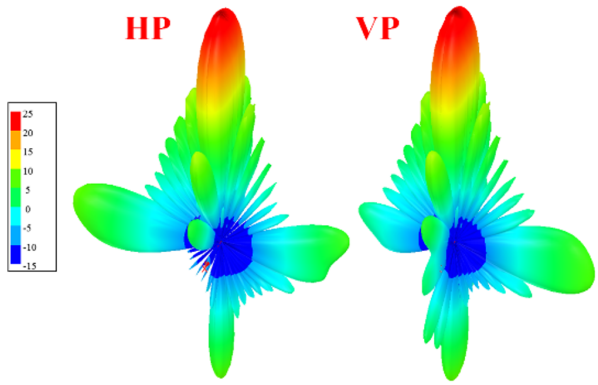

Fig. 18: 3-D radiation pattern of large-scale MIMO antenna array when excitation in horizontal and vertical polarization modes

Fig. 18 illustrates the 3-D radiation pattern of the large-scale MIMO antenna array when excitation in both horizontal and vertical polarization modes.

When exciting all ports in either horizontal or vertical polarization modes, the proposed antenna array can achieve a main beam with a maximum real gain of ∼22 dBi. A comparison table of some MIMO antennas designed for 5G base stations is shown in Table 2. The proposed antenna array is larger than the previously proposed antennas, but the gain is improved significantly.

3. Conclusion

With many advantages of low profile, flat array, wide operating bandwidth, low mutuality, this large-scale MIMO antenna array can be applied to the current generation of 5G mobile base stations.

TABLE 2: Comparison table of some MIMO antennas designed for 5G base stations

MIMO Antenna	Frequency	Substrate	Dimension	Gain
PANG Xingdong [8]	5.7-5.9 GHz	TLX-8, ϵ_r=2.55, h=1 mm	320 mm × 860 mm × 1mm	10 dBi
Mengting Li [9]	3.5 GHz	FR-4, ϵ_r=4.4, h=1 mm	101 mm × 170 mm × 14 mm	6.8 dBi
Donglin He [10]	0.69–0.96 GHz, 1.8–2.7 GHz, 3.3–3.8 GHz	RF-10, ϵ_r=10.2, h=0.638 mm	300 mm × 300 mm × 77 mm	8.2 dBi
Proposed antenna	3,3 – 3,8 GHz	FR-4, ϵ_r=4.4, h= 4.2 mm,	264 mm × 640 mm × 4,2 mm	22 dBi

Acknowledgment

This research is funded by Hanoi University of Science and Technology (HUST) under project number T2021-TT-005.

References

[1] P. Xingdong, H. Wei, Y. Tianyang, and L. Linsheng, "Design and implementation of an active multibeam antenna system with 64 rf channels and 256 antenna elements for massive mimo application in 5g wireless communications," *China Commun.*, vol. 11, no. 11, pp. 16–23, Nov. 2014.

[2] Y. Zeng, R. Zhang, and Z. N. Chen, "Electromagnetic lens-focusing antenna enabled massive mimo: Performance improvement and cost reduction," *IEEE J. Sel. Areas Commun.*, vol. 32, no. 6, pp. 1194–1206, Jun. 2014.

[3] I. Tzanidis *et al.*, "Patch antenna array configuration for application in fd-mimo systems," *Proc. IEEE Antennas Propag. Soc. Int. Symp.*, pp. 2241–2242, Jul. 2013.

[4] S. Gao and A. Sambell, "Low-cost dual-polarized printed array with broad bandwidth," *IEEE Trans. Antennas Propag.*, vol. 52, no. 12, pp. 3394–3397, Dec. 2004.

[5] W. Yun and Y.-J. Yoon, "A wide-band aperture coupled microstrip array antenna using inverted feeding structures," *IEEE Trans. Antennas Propag.*, vol. 53, no. 2, pp. 861–862, Feb. 2005.

[6] K.-L. Wong and T.-W. Chiou, "Cfinite ground plane effects on broad-band dual polarized patch antenna properties," *IEEE Trans. Antennas Propag.*, vol. 51, no. 4, pp. 903–904, Apr. 2003.

[7] H. Wong, K.-L. Lau, and K.-M. Luk, "Design of dual-polarized l-probe patch antenna arrays with high isolation," *IEEE Trans. Antennas Propag.*, vol. 52, no. 1, pp. 45–52, Jan. 2004.

[8] P. Xingdong, H. Wei, Y. Tianyang, and L. Linsheng, "Design and implementation of an active multibeam antenna system with 64 rf channels and 256 antenna elements for massive mimo application in 5g wireless communications," *China Communications*, vol. 11, no. 11, pp. 16–23, Nov. 2014.

[9] M. Li, X. Chen, A. Zhang, Ahmed, and A. Kishk, "Dual-polarized broadband base station antenna backed with dielectric cavity for 5g communications," *IEEE Antenna Propagation Letters*, vol. 18, no. 10, pp. 2051–2055, Oct. 2019.

[10] D. He, Y. Chen, and S. Yang, "A low-profile triple-band shared-aperture antenna array for 5g base station applications," *IEEE Transactions on Antennas and Propagation*, vol. 70, no. 4, pp. 2732–2739, Apr. 2022.

Hien Doan Thi Ngoc has done her PhD in the School of Electronic and Telecommunication, Hanoi University of Science and Technology. She has graduated in Telecomunication Engineering and masters in information processing and communication fromHanoi University of Science and Technology, Vietnam. Her research focuses on the Antenna and Communication.